LETTER Communicated by Nancy Kopell

Synchronization in Relaxation Oscillator Networks with Conduction Delays

Jeffrey J. Fox
Department of Physics, Cornell University, Ithaca, NY 14853, U.S.A.

Ciriyam Jayaprakash
Department of Physics, The Ohio State University, Columbus, Ohio 43210, U.S.A.

DeLiang Wang
Department of Computer and Information Science and Center for Cognitive Science, The Ohio State University, Columbus, Ohio 43210, U.S.A.

Shannon R. Campbell
Physical Optics Corporation R & D Division, Torrance, California 90505, U.S.A.

We study locally coupled networks of relaxation oscillators with excitatory connections and conduction delays and propose a mechanism for achieving zero phase-lag synchrony. Our mechanism is based on the observation that different rates of motion along different nullclines of the system can lead to synchrony in the presence of conduction delays. We analyze the system of two coupled oscillators and derive phase compression rates. This analysis indicates how to choose nullclines for individual relaxation oscillators in order to induce rapid synchrony. The numerical simulations demonstrate that our analytical results extend to locally coupled networks with conduction delays and that these networks can attain rapid synchrony with appropriately chosen nullclines and initial conditions. The robustness of the proposed mechanism is verified with respect to different nullclines, variations in parameter values, and initial conditions.

1 Introduction

Synchronous neural activity has been observed in many parts of the brain and across the two hemispheres (Singer & Gray, 1995; Phillips & Singer, 1997; Keil, Mueller, Ray, Gruber, & Elbert, 1999). Neural synchrony arises quickly, within one to two periods of stimulus onset. It is often precise, with zero or at most a few milliseconds difference in firing times, and is observed over a considerable distance of the cortex (e.g., 14 mm in the primate motor cortex). This is quite remarkable given that significant delays occur during nerve conduction; for instance, the conduction speed in local cortical circuits

is less than 1 m/sec (Kandel, Schwartz, & Jessell, 1991; Murakoshi, Guo, & Ichinose, 1993). With the commonly reported 40 Hz oscillation frequency, such a conduction speed implies that connected neurons that are 1 mm apart have a time delay of more than 4% of the period of oscillation.

Extensive experimental findings of neural synchrony have stimulated much research in understanding how populations of oscillators can achieve synchrony. Such studies reveal that locally coupled oscillator networks with excitatory coupling and no conduction delay can reach global synchrony across the network. In particular, relaxation oscillators, which link directly to neuronal models of spike generation (FitzHugh, 1961; Nagumo, Arimoto, & Yoshizawa, 1962; Morris & Lecar, 1981), have been shown to synchronize rapidly with local coupling (Somers & Kopell, 1993; Terman & Wang, 1995).

A number of studies have examined the effects of time delays in oscillator networks and reveal a diverse and interesting range of behaviors. For example, in a network of identical phase oscillators with local excitatory coupling, the inclusion of a time delay in the interactions decreases the frequency (Niebur, Schuster, & Kammen, 1991). Analysis of pulse-coupled oscillators indicates that time delays together with excitatory coupling do not lead to synchronization in a pair of oscillators; however, if the coupling is inhibitory, a pair of oscillators can be synchronous (van Vreeswijk, Abbott, & Ermentrout, 1994; Ernst, Pawelzik, & Geisel, 1995). Ernst et al. (1995) also examined, through computer simulations, networks of pulse-coupled oscillators with all-to-all connections and time delays. They found that if the coupling is excitatory, then groups of synchronous oscillators spontaneously arise and decay; if the coupling is inhibitory, several clusters of stable synchronous oscillators can form. Campbell and Wang (1998) found that a network of locally coupled relaxation oscillators with delayed excitatory coupling exhibits loose synchrony, whereby the oscillators that are directly coupled converge to a phase separation less than or equal to the time delay.

More biologically realistic models of neural oscillators also exhibit synchrony when coupled with time delays. König and Schillen (1991) reported that a system of Wilson-Cowan oscillators becomes synchronous, and time delays are important for the synchronous behavior. Traub, Whittington, Stanford, and Jefferys (1996) described a model of cortical circuitry in which synchrony in a network of neurons is observed with time-delay coupling and the synchronous behavior is linked to a specific firing pattern of interneurons—the so-called spike doublets. Their numerical findings have inspired Ermentrout and Kopell (1998) to analyze a similar but simplified system with a pair of local circuits, each consisting of one excitatory unit (E) and one inhibitory unit (I). They showed, by using $E \to I$ and $I \to E$ connections, that the model, due to the presence of doublets in inhibitory units, can synchronize with significant time delays.

Despite the studies on time delays in oscillator networks, it remains an interesting problem how synchrony with zero phase lag can be achieved efficiently in locally coupled networks with time delays. In this article we

propose a different mechanism for achieving rapid synchrony in locally coupled relaxation oscillators. The key idea is that this can be accomplished by choosing the nullclines of individual oscillators appropriately. We study the case of two-coupled oscillators approximately analytically in the next section; this enables us to derive a formula that shows how an appropriate choice of the nullclines can be made and allows us to estimate the speed of convergence to synchrony. We have verified the analytical approximations by numerical simulations of the two-oscillator system. To establish the viability of our mechanism, we have studied one-dimensional (1D) and two-dimensional (2D) arrays of oscillators numerically. For time delays, on the order of 10% of the period of the single uncoupled oscillator and a spread of initial phases synchrony is achieved in a few periods in most cases. To demonstrate the wider applicability of this mechanism, different choices for the nullclines (linear, cubic, exponential, etc.) have been tested; provided the parameters are chosen according to the condition derived in the two-oscillator case, our mechanism is operative. In the case of the step function, there is no synchrony, as was shown earlier (Campbell & Wang, 1998), and the sigmoid function is not effective. We also discuss the effect of different initial conditions and offer some remarks in the case of inhomogeneous time delays with a spread. Thus, we provide a different mechanism for achieving synchrony in locally coupled oscillators with time delays; the models inspired by Traub et al. (1996) exploit an adjustment of timing structure via doublets using additional circuitry, while we use the choice of the intrinsic nullclines to accomplish the same result.

We describe our oscillator system in the next section and then analyze a pair of oscillators. Subsequently, we compare our analytical results with numerical simulations and examine synchrony in 1D and 2D oscillator networks. Further discussions are given in the last section.

2 Model Definition

For our study, we use relaxation oscillators similar to those defined by Terman and Wang (1995). Each oscillator i is described by the following equation,

$$\dot{x}_i = 3x_i - x_i^3 - y_i + S_i \tag{2.1a}$$

$$\dot{y}_i = \varepsilon(f(x_i) - y_i), \tag{2.1b}$$

where x_i is the excitatory variable, y_i is the inhibitory variable, and S is an excitatory coupling term. When ε is chosen small and there is no coupling, the equation corresponds to a standard relaxation oscillator (Wang, 1999). The x-nullcline of the oscillator is a cubic (see Figure 1). In the singular limit ($\varepsilon \to 0$), the orbit of the oscillator is determined by this nullcline. The oscillator rapidly alternates between the active phase of high x activity and the silent phase of low x activity (see Figure 1).

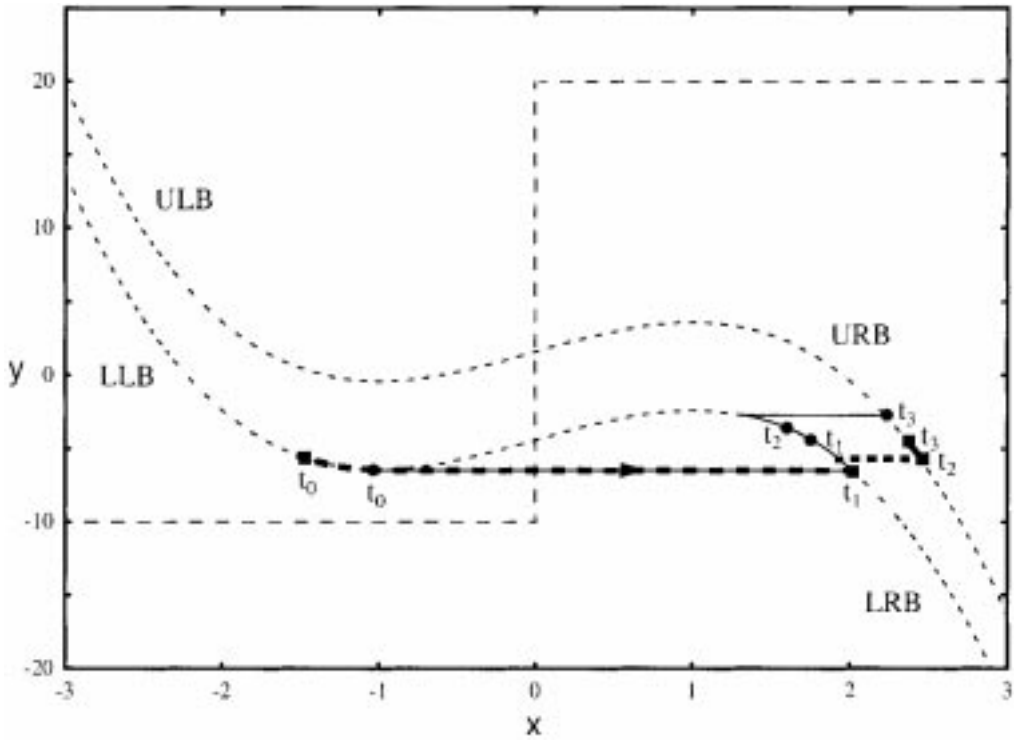

Figure 1: Loose synchrony with a step function y-nullcline. The two oscillators are indicated by a circle dot and a square dot, respectively, at four time instants. The oscillators move on the lower cubic when coupling is not activated. When an excitation takes effect, the oscillators move along the upper cubic. LLB, lower left branch; LRB, lower right branch; ULB, upper left branch; URB, upper right branch. Other notations are described in the text.

When the coupling is activated, the cubic is moved up vertically by an amount equal to the coupling strength (Somers & Kopell, 1993). An oscillator moves along the lower cubic unless it receives an excitation from a neighboring oscillator; in this case, it moves along a higher cubic (see Figure 1). The speed with which the oscillator moves along its cubic is determined by its distance to the y-nullcline, given by $f(x)$. By choosing the form of $f(x)$, one can control not only the dynamics of the oscillator but also the synchronizing behavior of an oscillator system. This observation leads to our mechanism for achieving synchrony in a locally coupled network with conduction delays.

We study 1D or 2D locally coupled networks, where each oscillator is coupled only with its nearest neighbors. The coupling term S in equation 2.1a is given by

$$S_i = \sum_k W_{ik} S_\infty(x_k(t-\tau)) \tag{2.2}$$

$$S_\infty = 1/(1+\exp[-K(x-\theta)]), \tag{2.3}$$

where τ is the conduction delay for a signal to travel from one oscillator to its neighbors, K is a parameter for the sigmoid function S_∞, and θ is a threshold an oscillator needs to reach in order to influence the activity of its neighbors. W_{ik} is the strength of the synaptic coupling from oscillator k to oscillator i. The coupling is local; thus, W_{ik} is zero unless i and k are adjacent. To eliminate boundary effects, we normalize the connection weights to each oscillator so that $W_{ik} = \alpha/N_i$, where N_i is the number of neighbors coupled to i and α is a constant (see Wang, 1995). In this article, N_i can be one, two, three, or four depending on the location of i and the dimensionality (1D or 2D) of the network.

3 Analysis

To illustrate better how the y-nullcline controls the dynamics of the network, we analyze the two-oscillator case in the singular limit. Let us first consider a special case with the y-nullcline being a step function, which helps to explain several terms and the consequences of introducing time delays. This case has been extensively analyzed by Campbell and Wang (1998), who conclude that such a system will reach only loose synchrony (see section 1). Figure 1 illustrates such a scenario with only two cubics to consider, one above the other by a constant α. LLB and LRB stand for the lower left branch and the lower right branch, respectively, and ULB and URB the upper left branch and the upper right branch, respectively. In Figure 1, the two oscillators are denoted by a circular dot (leading one) and square dot (trailing one), and the trajectory of the leading one is denoted by a thin, solid curve and that of the trailing one by a thick, dashed curve. Let the two oscillators start on LLB at t_0, when the leading oscillator is just ready to jump to LRB. Let Γ be the initial phase separation, or the time the trailing oscillator takes to catch up to the leading one if the latter is held stationary. Note that Γ does not change when both oscillators are on the same branch (Somers & Kopell, 1993), because when the oscillators remain on the same cubic, both traverse the same path. Assume that $\Gamma < \tau$. In this case, the trailing oscillator jumps to LRB at t_1, before the delayed excitation from the leading one takes effect. As a result, at t_1, the phase separation between the two oscillators is still Γ. Both oscillators travel on LRB until t_2, when the delayed excitation from the leading oscillator takes effect, which makes the trailing one hop to URB (see Figure 1). Note that because of the step y-nullcline, two oscillators of the same y value, one on URB and another on LRB, move with the same speed in the y direction. At t_3, the delayed excitation from the trailing oscillator to the leading one takes effect and makes the leading oscillator hop to URB. Now both oscillators are on URB, and their phase separation is still Γ because of the step y-nullcline. Indeed, their phase separation remains Γ throughout the entire limit cycle (Campbell & Wang, 1998). Thus, phase compression—the reduction of initial phase separation—does not occur when $\Gamma < \tau$.

This example clearly shows that time delays introduce a major change in the behavior of the system, since it is well known that two-coupled relaxation oscillators with a step y-nullcline rapidly synchronize to zero-phase separation (Somers & Kopell, 1993; Terman & Wang, 1995). Without a time delay, the leading oscillator, when it jumps to the right branch, induces the trailing one to jump immediately, provided that Γ is not too large (see Figure 1). Phase compression occurs during the simultaneous jumping process, because the phase separation after both jump to the right branch is smaller compared to before the jumping, when both are on the left branch.

Since a step function has zero slope, the analysis also illustrates that the y-nullcline must have some slope in order to achieve exact synchrony. Then the oscillators with the same y value have different speeds on different cubics. The following analysis provides an idea of precisely what slope is necessary for fast synchronization.

For this analysis, we make two assumptions. First, the y-nullcline is lower than both cubics along their left branches and higher along their right branches, so that any intersections between the two nullclines occur only along the middle branches of the cubics. Second, the two oscillators are initially on LLB.

We follow the technique used by Somers and Kopell (1993) and Mirollo and Strogatz (1990) to find a return map for Γ, that is, the phase separation of the two oscillators after one complete period as a function of the initial phase separation. To find this return map, we first determine Γ', the phase separation after both have just jumped from LLB to URB.

Denote time $t = 0$ when the leading one has just reached the left knee of LLB (see Figure 2). At time $t = \Gamma$, the trailing one jumps from LLB to LRB. Next, at $t = \tau$, the delayed excitation from the leading oscillator reaches the trailing one, causing it to hop from b on LRB to b' on URB (see Figure 2). Note that the trailing oscillator has traveled for a time $\tau - \Gamma$ on LRB. Finally, at time $t = \tau + \Gamma$, the delayed excitation from the trailing oscillator reaches the leading one, causing it to hop from a on LRB to a' on URB. At time $\tau + \Gamma$, the phase separation between the two oscillators is denoted by Γ'. To find Γ', we first note that the trailing oscillator has spent a time Γ on URB before the cubic of the leading oscillator is raised at point a. During this time, the trailing oscillator has moved from b' to a point denoted by a square dot in Figure 2. Clearly, Γ' is the time it takes for the oscillator to move from this point to a'. Thus, we can write

$$\Gamma' + \Gamma = t_{b'-a'}, \tag{3.1}$$

where $t_{b'-a'}$ is the time it takes an oscillator to move from b' to a' along URB. If we go through similar arguments for the jumps from the active phase to the silent phase that bring the oscillators back to LLB, we find

$$\Gamma'' + \Gamma' = t_{B-A}. \tag{3.2}$$

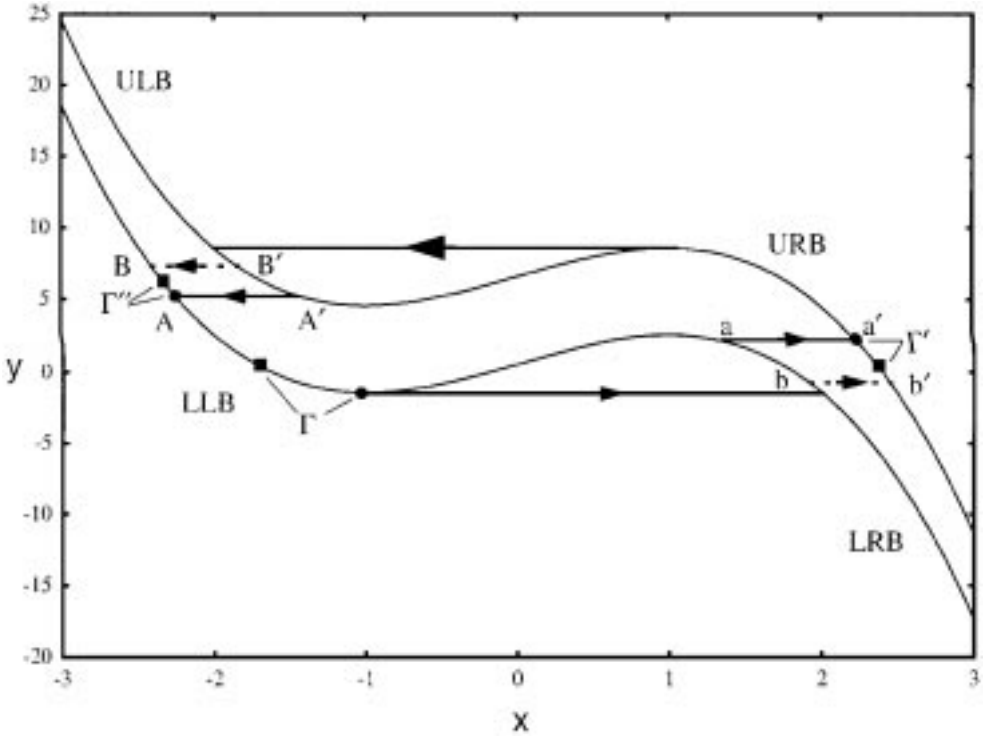

Figure 2: The two-oscillator case. Each pair of circle and square dots represents the locations of the two oscillators at a specific time. The lower-left pair represents the initial phase separation (Γ), the right pair represents the phase separation (Γ') after one jump, and the upper-left pair represents the phase separation (Γ'') after two jumps (one up and one down). Other labels are described in the text.

Here t_{B-A} is the time it takes an oscillator to move from point B to A (see Figure 2), where the trailing and the leading oscillators hop down from ULB to LLB, respectively.

Finally, the return map can be rewritten as

$$\Gamma'' = \Gamma - (t_{b'-a'} - t_{B-A}), \tag{3.3}$$

and writing the times $t_{b'-a'}$ and t_{B-A} as integrals, we have

$$\Gamma'' = \Gamma - \left(\int_{b'}^{a'} \frac{dy}{\dot{y}} - \int_{B}^{A} \frac{dy}{\underline{\dot{y}}} \right), \tag{3.4}$$

where the lower bar in y indicates the lower cubic.

Now, let $h_R(y)$ and $h_L(y)$ denote the x coordinates of LRB and LLB. Then, $h_R(y-\alpha)$ and $h_L(y-\alpha)$ correspond to those of URB and ULB. Thus, we have

$$\Gamma'' = \Gamma - \left(\int_{b'}^{a'} \frac{dy}{\varepsilon \left(f(h_R(y-\alpha)) - y \right)} - \int_{B}^{A} \frac{d\underline{y}}{\varepsilon \left(f(h_L(y)) - y \right)} \right). \quad (3.5)$$

Note that in the singular limit, the y coordinates of points a', b', A', and B' are the same as those of points a, b, A, and B, respectively. In the limit cycle, let $t = 0$ denote the origin in time when the leading oscillator is at the lowest point on LRB and its y coordinate is thus $y(t = 0)$. As discussed earlier, at b', the trailing oscillator has traveled for a time $\tau - \Gamma$ on LRB, and hence, its y coordinate is $y(\tau - \Gamma)$. At a, when the leading oscillator receives an excitatory signal from the trailing one, it has traveled for time $\tau + \Gamma$ starting from the lowest point, and thus, the y coordinate of a' is simply $y(\tau + \Gamma)$. This allows us to rewrite the limits of the first integral in equation 3.5. We can similarly start the clock at the highest point of ULB and let its y coordinate be denoted by $\underline{y}(t = 0)$ and rewrite the limits of the second integral. Hence, we have

$$\Gamma'' = \Gamma - \left(\int_{y(\tau-\Gamma)}^{y(\tau+\Gamma)} \frac{dy}{\varepsilon \left(f(\dot{h}_R(y-\alpha)) - y \right)} - \int_{\underline{y}(\tau-\Gamma')}^{\underline{y}(\tau+\Gamma')} \frac{d\underline{y}}{\varepsilon \left(f(h_L(\underline{y})) - \underline{y} \right)} \right). \quad (3.6)$$

Finally, we expand both integrals for the case $\Gamma < \tau$ and $\Gamma' < \tau$ using the formula for differentiating an integral with respect to a parameter (Courant, 1988). If

$$G(x) \equiv \int_{f_1(x)}^{f_2(x)} F(y, x) dy,$$

then

$$\frac{dG(x)}{dx} = \int_{f_1(x)}^{f_2(x)} \frac{\partial F(y, x)}{\partial x} dy + \frac{df_2(x)}{dx} F(f_2(x), x) - \frac{df_1(x)}{dx} F(f_1(x), x).$$

Using this for Γ' given by

$$\Gamma' = -\Gamma + \int_{y(\tau-\Gamma)}^{y(\tau+\Gamma)} \frac{dy}{\varepsilon (f(h_R(y-\alpha)) - y)},$$

and expanding we obtain to leading order in Γ,

$$\Gamma' \approx \Gamma(-1 + 2R/R_\alpha),$$

where we define

$$R = [f(h_R(y)) - y]|_{t=\tau}$$
$$R_\alpha = [f(h_R(y-\alpha)) - y]|_{t=\tau}.$$

Similarly, we obtain

$$\Gamma'' \approx \Gamma'(-1 + 2L_\alpha/L)$$

with

$$L = [f(h_L(\underline{y})) - \underline{y}]|_{t=\tau}$$
$$L_\alpha = [f(h_L(\underline{y} - \alpha)) - \underline{y}]|_{t=\tau}.$$

Together they lead to the following key equation:

$$\Gamma'' \approx \Gamma(1 - 2R/R_\alpha)(1 - 2L_\alpha/L). \tag{3.7}$$

Thus, to eliminate the first-order term in the expansion of Γ'' in powers of Γ, we need R, the vertical distance from the y-nullcline to the point $y(\tau)$ on LRB, to be one-half of R_α, the distance from the y-nullcline to the point on URB corresponding to the same y value; or a similar condition must hold on the left branches. If $f(x)$ is such that this $1/2$ ratio holds for a larger and larger region around $y(\tau)$, then more and more terms in the expansion of Γ'' drop out. If the ratio holds for the entire right (or left) branch, Γ'' goes immediately to zero after only one jump to the active phase. A symmetric y-nullcline produces equal compression for both left-to-right and right-to-left jumps. These observations provide a guide to the choice of the nullclines for efficient synchronization.

We note that this first-order result agrees with the findings of Campbell and Wang (1998) in the case that $f(x)$ is a step function; the ratio of vertical distances to the y-nullcline is one across the entire branch, yielding $\Gamma'' = \Gamma$, or no compression once Γ is less than τ. Equation 3.7 is clearly useful for establishing the stability of a synchronous solution, as well as for estimating the speed of convergence to synchrony once a particular y-nullcline is chosen.

We can also employ this analysis to determine the effects of asymmetric time delays. That is, the conduction delay from one oscillator to the other differs by an amount δ from that in the opposite direction. In this case, the system will not reach zero-phase synchrony. One can show that for a symmetric y-nullcline chosen such that the first-order term in equation 3.7 is negligible, the system will reach a stable phase difference equal to $\delta/2$, a result that we have confirmed numerically. In order to draw a comparison, we have extended the analysis of Ermentrout and Kopell (1998). If we let the delay from circuit 1 to circuit 2 be δ, and let the delay from circuit 2 to circuit 1 be $\delta + \delta'$, then one can choose parameters so that the system reaches a stable fixed point with a phase difference $\delta'/2$. Thus, our model with fewer parameters produces similar results.

One can find an expression similar to equation 3.6 for the return map if Γ and Γ' are larger than τ. However, this map appears more difficult to analyze, and we content ourselves with a numerical study in the next section.

Finally, we note that in some cases, we can provide an explicit expression of a y-nullcline that produces synchronization after only one jump from the silent phase to the active phase. Let us denote by d the mean difference in x values ($h_R(y-\alpha) - h_R(y)$ in our earlier notation) between LRB and URB for the relevant range of y coordinates. We note that for the cubic x-nullcline considered in this article, this difference does not vary much. In such cases the y-nullcline given by an exponential function $f(x) = C \bullet 2^{x/d}$ for a constant C produces a $1/2$ ratio between the y-coordinate of the y-nullcline for a point on LRB and that of the corresponding point on URB with the same y value. Because for a given x along the right branches, the y-coordinate of the y-nullcline is much greater than that of the x-nullcline, the latter can be ignored in the calculations of R and R_α. Thus, this choice of $f(x)$ approximately satisfies the $1/2$ ratio between R and R_α, and produces essentially immediate synchronization after one jump.

4 Numerical Simulation

The second part of our study consists of numerical simulations. We relate our numerical results for the two-oscillator case to our analytical results. The bulk of the section describes our results for 1D and 2D networks. We discuss various types of y-nullclines that can produce fast synchrony and the robustness of this mechanism.

We use the fourth-order Runge-Kutta method (Press, Teukolsky, Vetterling, & Flannery, 1992) adapted to time delays to solve our equations, typically with a time step of 0.01; smaller time steps have been used to verify our numerical results. A fifth-order Lagrange interpolation formula (Abramowitz & Stegun, 1964) is used to determine the required intermediate values of x. Unless otherwise noted, the results discussed in this section are obtained using the following set of parameters: $\varepsilon = 0.02$, $\tau = 2.0$, $\alpha = 6.0$, $K = 50.0$, and $\theta = -0.5$. This value of τ is about 10% of the oscillation period for an uncoupled oscillator. For the y-nullcline, we used $f(x) = 8x^3 + 5$ (see Figure 6).

4.1 Two-Coupled Oscillators. We first describe the two-oscillator case. With the above parameter values, using numerically obtained values for $x(\tau)$ and $y(\tau)$, we find that the coefficient in the first-order expansion for Γ'' in equation 3.7 is approximately 0.0116. In Figure 3A, we show a graph of $\Gamma''(\Gamma)$ obtained both numerically and analytically. Note that for $\Gamma < 1$, the analytical approximation is reasonably accurate. For Γ larger than 1, the higher-order terms begin to dominate, and the first-order approximation is no longer good. The asymptotic slope for the numerically obtained data is about 0.013. This agrees with the predicted result to about 12%. We have obtained comparable or better agreement for other values of ε.

Figure 3B shows the numerically obtained return map for Γ, ranging from zero to a value equal to the time needed to traverse the entire LLB. In

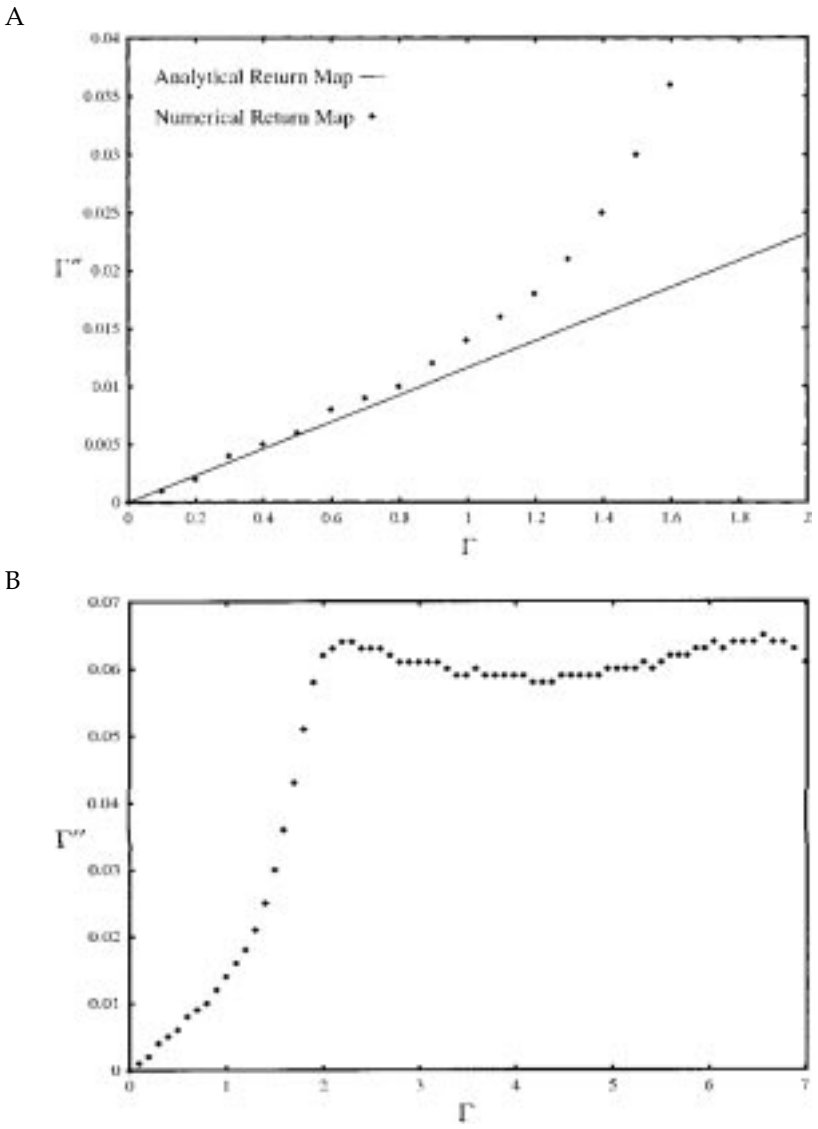

Figure 3: Return maps for the two-oscillator case, with $\tau = 2.0$. (A) Numerical and analytical return maps for $\Gamma < \tau$. The dots are numerically obtained data points, and the line is the analytical approximation. Note that for Γ small, the numerical return map is approximately linear and agrees well with the analytical map. (B) Numerically obtained return map for a large range of Γ.

this and all the following cases, when we refer to positions on a particular branch, they are limited to the portion of the branch within the limit cycle of the oscillation (see Figure 2). Note the dramatic change in the return map for $\Gamma > \tau$. Although we do not have an analytical calculation for the general case, a qualitative understanding follows from the analysis of Campbell and Wang (1998) done in a similar situation (see also Somers & Kopell, 1993). If Γ is larger than τ, then after the leading oscillator jumps to the active phase, the

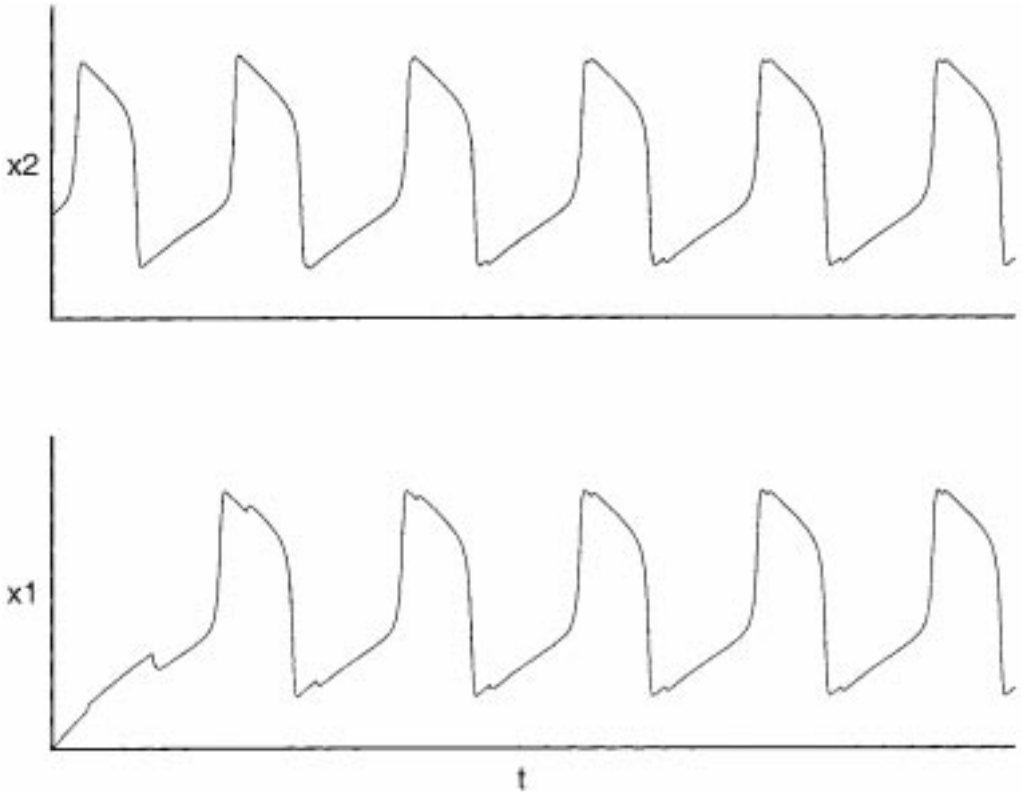

Figure 4: Synchronization of two-coupled oscillators. The oscillators start at the two ends of LLB with $x_1 = -2$ and $x_2 = -1$.

trailing oscillator still spends some time in the silent phase after it receives excitation from the leading one and hops to ULB. Thus, the two oscillators travel in opposite directions on the different nullclines during this time, resulting in dramatic compression of their phase separation. The return map indicates that the two-oscillator case always converges to synchrony.

Figure 4 illustrates the synchronization process in the two-oscillator case. The two oscillators start at the two extreme ends on LLB. Also, for purposes of illustration, the coupling strength α is much reduced to 1.0 so that synchrony does not occur as fast.

4.2 One-Dimensional Arrays. We now describe our numerical results for 1D arrays. Table 1 shows the average time to synchrony in terms of the number of periods for several array sizes. The results are obtained by averaging over 25 trials. To determine initial conditions, we randomly select y values between the highest point on LLB ($y = 2$) and a point on LLB chosen so that the spread of initial conditions is 43% of the total time to traverse LLB (we explain this choice below). We define a network as synchronized if the maximum phase separation between any two oscillators is less than 3%

Table 1: Average Rates of Synchrony in 1D Arrays.

	Array Size				
	2	4	8	16	32
Average periods to synchrony	1.0	1.08	3.24	6.16	8.36

of the total period of an oscillator. For smaller arrays, synchrony is always quite fast. For larger arrays (larger than 10), we find that certain initial conditions lead to very slow synchrony. After studying these cases more carefully, we find that slow synchrony is due to the presence of two or more domains, or blocks of connected oscillators within each of which all have nearly the same phase. These domains result from the topology of 1D nearest-neighbor coupling. If the relative phase between two such domains is large, slow synchrony results because of the limited connectivity of the network. As we discuss below, the domain effects in 2D arrays are much less severe due to increased network connectivity; longer-range couplings are also expected to suppress domain effects and accelerate synchrony.

We have explored in greater detail cases with limited spread of randomly chosen initial conditions. We start all the oscillators in a simulation in a region of LLB. This region represents a spread of initial phases equal to 43% of the total time to traverse LLB. The specific percentage (43%) is empirically obtained so that the narrowing of the initial phase spread eliminates most of the slow synchrony cases. However, even for these initial conditions, about 1 in 25 trials has time to synchrony greater than 20 periods for arrays of size 8 or larger. As one further limits the range of initial conditions, the initial degree of synchrony is higher and higher. Thus, the time to synchrony can become arbitrarily small. Figure 5 shows a typical simulation with 20 oscillators, whose initial phases spread over the time to traverse LLB subtracted by τ. In this figure a dot in the ith row represents the time at which the ith oscillator jumps to the active phase.

To test the robustness of our model, we conducted simulations with different choices for y-nullclines. As shown in Figure 6, we have tested sigmoid, linear, cubic, exponential, and hyperbolic sine functions (some curves in Figure 6 are shifted vertically when used in simulations). We find that all of these functions except the sigmoid can yield rapid synchrony for appropriately chosen parameters. In fact, this is predicted by equation 3.7. According to the equation, to produce fast synchrony, the distance to a y-nullcline from the right-most point on LRB should be roughly half that from the corresponding point on URB with the same y-coordinate (see Figure 2). Thus, one expects that functions with smaller slopes, such as sigmoids, synchronize with a slower rate than functions with greater slopes, such as cubics. Also, equation 3.7 shows that nullclines that are symmetric about the

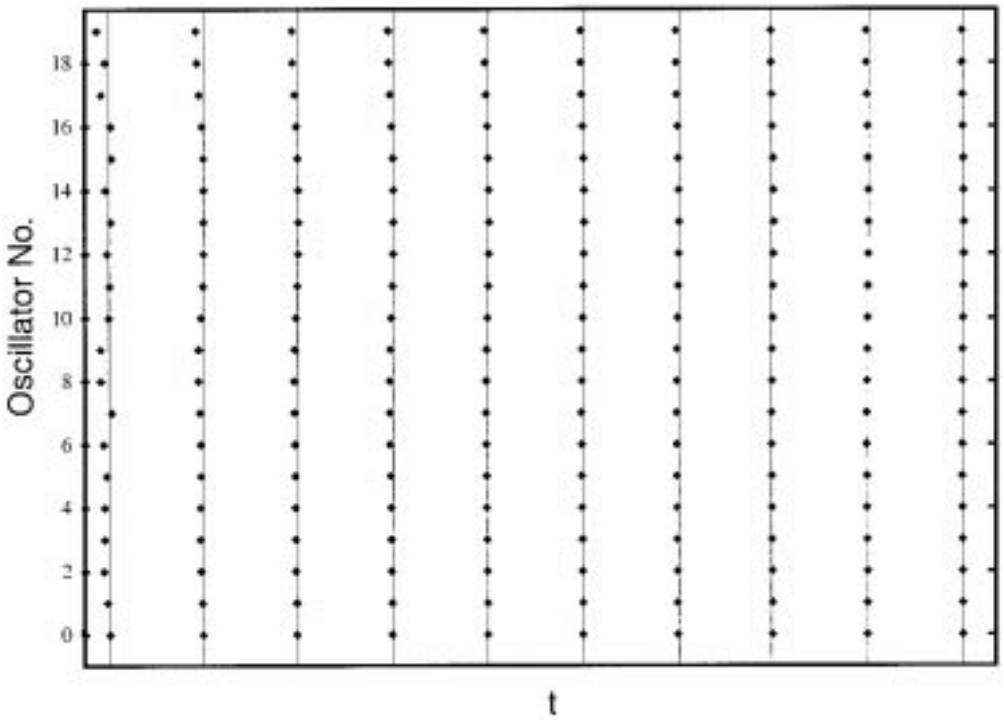

Figure 5: Synchronization in a 1D array of 20 oscillators. The horizontal axis represents time, and the vertical axis oscillator positions in the array.

origin produce convergence to synchrony for both jumping up and jumping down. Thus, we predict that symmetric functions, such as hyperbolic sines, synchronize with a faster rate than asymmetric ones, such as exponential functions. This is indeed what we have observed in simulations.

With the y-nullcline fixed to a cubic function, we have also checked for robustness with respect to parameter changes. We find that varying the time delay τ by 20% has little effect on the behavior of the system. Similarly, changing the parameters of a cubic y-nullcline does not affect the network behavior. Finally, we test how the network responds to inhomogeneous time delays. To do this, we vary the delays between oscillators by a random variable up to 5% width of the time delay; large inhomogeneities in conduction delays prevent synchronization, as expected. Note that in this case, the time delay from oscillator i to j is generally different from that from j to i. We find that the system does not converge to zero phase-lag synchrony with such an inhomogeneity. However, the inhomogeneous system does converge to satisfy the 3% synchrony condition discussed earlier, with a rate similar to that of the corresponding homogeneous system. Other networks, such as those that make use of spike doublets in inhibitory units (Ermentrout & Kopell, 1998), are also unable to reach zero phase-lag synchrony in the presence of such inhomogeneity.

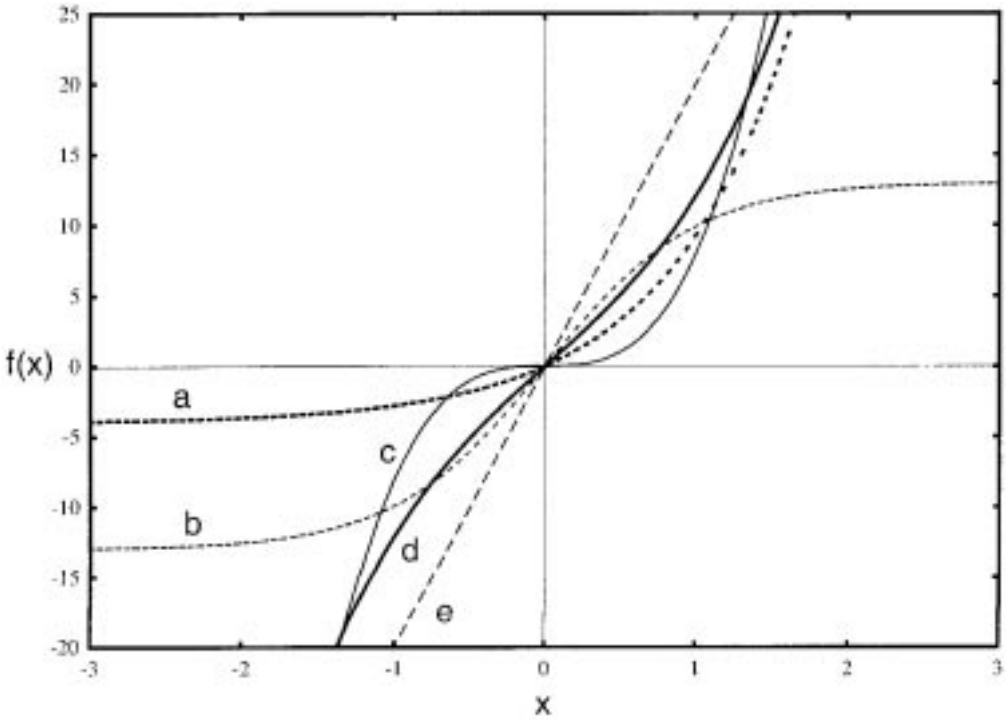

Figure 6: Plot of several y-nullclines that have been studied, where a is an exponential curve ($f(x) = 4 \bullet 2^{2x} - 4$), b is a sigmoid curve ($f(x) = 13 \bullet \tanh(0.7x)$), c is a cubic curve ($f(x) = 8x^3$), d is a linear curve ($f(x) = 20x$), and e is a sinh curve ($f(x) = 8 \sinh(x \bullet \ln 4)$).

4.3 Two-Dimensional Networks. In the 2D case, each oscillator is connected with its four nearest neighbors with open boundaries. As mentioned earlier, synchronization in 2D networks with random initial conditions is less susceptible to domain effects. We have studied 10×10 networks because the maximum distance between any two oscillators is the same as in a 1D 20-oscillator array. With the same initial conditions used to produce Table 1, the average time to synchrony over 25 trials in the 20 oscillator array is 6.52 periods. For a 10×10 network, using the same spread of initial conditions, the average time to synchrony over the same number of trials is 3.36 periods. In these trials, the longest time to synchrony is 9 periods.

We have also studied other initial conditions. We first split the network into two 5×10 blocks of oscillators: one block with all the oscillators beginning at the top of LLB and the other with all the oscillators near the bottom of LLB. This condition causes very slow synchrony (greater than 40 periods). However, the condition represents a worst case due to its similarity to 1D arrays. In another condition, we start all the oscillators in a 4×4 square at the center of the network at one extreme of the left branch, and all other oscillators at the other extreme. This initial condition yields synchrony in 12

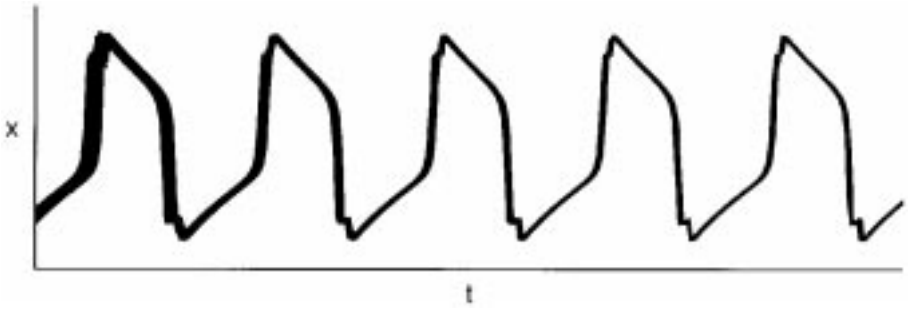

Figure 7: Synchronization in a 20 × 20 2D network. The horizontal axis represents time, and the vertical axis x activity. The activity of all 400 oscillators is superimposed.

periods. We expect that networks with greater connectivity, such as those in which connectivity is gaussian rather than nearest neighbor, show even faster synchrony.

Finally, we have tested a 20×20 network where each oscillator randomly starts in a rectangle that just bounds the limit cycles of all the oscillators (see Figure 2); in other words, each oscillator has an equal chance of falling into the silent phase or the active phase. In this case, the network still converges to synchrony, although the time to synchrony is generally greater than 20 periods.

Because of increased connectivity in 2D networks, we can use a spread of initial conditions over 71% of the time to traverse LLB. Note that the 71% initial spread is the maximum spread on LLB after the time delay is considered, which is about 29% of the time to traverse LLB. For a 20×20 array with these initial conditions, we find that an average time to synchrony is 12.36 periods, with the maximum time (out of 25 trials) of 23 periods. Figure 7 shows the synchronization process of a 20 × 20 network. The network in this case synchronizes after about 5 periods; the maximum phase separation between any two oscillators is less than the 3% period criterion.

5 Discussion

Our analysis shows that the synchronous solution can be stable for a pair of relaxation oscillators in the presence of conduction delays. We have derived an approximation for the rate of synchrony. This analysis indicates how to choose y-nullclines for relaxation oscillators to induce rapid synchrony. We have also examined asymmetric conduction delays between two oscillators. We find that small differences lead to a solution in which the phase separation between the oscillators is approximately half the difference of the two time delays; in other words, the system is nearly synchronous. Further, we have conducted numerical simulations in 1D and 2D oscillator networks.

Our simulations indicate that synchrony also occurs in these systems for a range of y-nullclines, initial conditions, parameters, and time delays. We have studied large phase separation in the initial conditions of the oscillators (40% of the time to traverse the left branch) and time delays up to 12% of the period of an uncoupled oscillator and find that our mechanism works for the given set of parameters. These systems also become nearly synchronous with inhomogeneous delays, analogous to the two-oscillator case. We have not studied much larger values of τ, particularly in cases where the sum of the time delay and the largest phase separation exceeds the time taken to traverse one of the branches.

Our study provides insights into the dynamics of relaxation oscillator systems with time delays. Fast synchronization does not depend on the exact form of a y-nullcline; it results as long as the 1/2 ratio approximately holds between the rates of motion on LRB and URB. A reasonably symmetric y-nullcline speeds up the process of synchronization further. We have described what initial conditions are appropriate to achieve rapid synchrony, as some special initial conditions can result in slower synchronization than others.

The set of y-nullclines displayed in Figure 6 includes the linear function used in the FitzHugh-Nagumo oscillator (FitzHugh, 1961; Nagumo et al., 1962) and the sigmoid function used in the Morris-Lecar oscillator (Morris & Lecar, 1981); both are relaxation oscillators and have been widely used as models of neuronal activity. How well networks of these oscillators synchronize with time-delay coupling depends on specific linear and sigmoid functions used. Qualitatively speaking, our analysis suggests that in the presence of conduction delays, linear y-nullclines should result in faster synchronization than sigmoid y-nullclines.

Previous studies examined coupled integrate-and-fire oscillators and found that synchrony can arise in the presence of time delays (van Vreeswijk et al., 1994; Ernst et al., 1995). These studies found that inhibitory connections are needed for synchronous solutions in the presence of time delays. Our mechanism for achieving synchronization in relaxation oscillators is quite different. Synchrony in our model relies on the fact that there are different rates of motion along the different nullclines of the system. Integrate-and-fire oscillators do not possess separate nullclines and thus cannot accommodate a mechanism like ours. In our system, the interaction is still excitatory, and the synchronous solution remains stable as time delays are introduced into the system, which does not occur in integrate-and-fire oscillator networks.

As analyzed by Ermentrout and Kopell (1998), oscillator models with delicate timing structure (i.e. spike doublets; see Traub et al., 1996) can also exhibit synchrony with time delays. Our model achieves a similar objective in a very different way. We do not use another circuitry to deal with time delays; the y-nullcline is an intrinsic part of a relaxation oscillator. As a result, our mechanism is simpler. On the other hand, our

mechanism is not as directly motivated biologically as that of Ermentrout and Kopell.

We conclude that synchrony exists in systems of locally coupled relaxation oscillators in the presence of conduction delays and with excitatory coupling. Our analysis reveals that y-nullclines can play an important role in synchronizing a locally coupled network of relaxation oscillators with conduction delays. A variety of y-nullclines have been tested and shown to yield rapid synchrony. Moreover, our result allows one to predict whether and how quickly a given y-nullcline produces synchrony. Given that relaxation oscillators have direct linkage to neuronal models, our analysis may help in understanding how synchrony arises in neural systems, where conduction delays are inevitable. Our insights into how to create appropriate conditions to achieve zero phase-lag synchrony may also be very useful in constructing and analyzing physical systems (Cosp, Madrenas, & Cabestany, 1999). Some opto-electronic systems and devices that operate at extremely high frequencies (Wirkus & Rand, 1997; Young et al., 1988) are modeled as coupled relaxation oscillators, and in these systems conduction delays can become a significant percentage of the oscillation period.

Acknowledgments

This work was supported in part by an NSF grant (IRI-9423312) and an ONR Young Investigator Award (N00014-96-1-0676) to D. L. W. C. J. acknowledges computer support from the Ohio Supercomputer Center.

References

Abramowitz, M., & Stegun, I. (Eds.). (1964). *Handbook of mathematical functions*. Washington, DC: U.S. Government Printing Office.

Campbell, S. R., & Wang, D. L. (1998). Relaxation oscillators with time delay coupling. *Physica D, 111*, 151–178.

Cosp, J., Madrenas, J., & Cabestany, J. (1999). A VLSI implementation of a neuromorphic network for scene segmentation. In *Proceedings of MicroNeuro* (pp. 403–408).

Courant, R. (1988). *Differential and integral calculus*. New York: Wiley.

Ermentrout, G. B., & Kopell, N. (1998). Fine structure of neural spiking and synchronization in the presence of conduction delays. *Proc. Natl. Acad. Sci. USA, 95*, 1259–1264.

Ernst, U., Pawelzik, K., & Geisel, T. (1995). Synchronization induced by temporal delays in pulse-coupled oscillators. *Phys. Rev. Lett., 74*, 1570–1573.

FitzHugh, R. (1961). Impulses and physiological states in models of nerve membrane. *Biophys. J., 1*, 445–466.

Kandel, E. R., Schwartz, J. H., & Jessell, T. M. (1991). *Principles of neural science* (3rd ed.), New York: Elsevier.

Keil, A., Mueller, M. M., Ray, W. J., Gruber, T., & Elbert, T. (1999). Human gamma band activity and perception of a Gestalt. *J. Neurosci., 19*, 7152–7161.

König, P., & Schillen, T. B. (1991). Stimulus-dependent assembly formation of oscillatory responses: I. Synchronization. *Neural Comp., 3*, 155–166.

Mirollo, R. E., & Strogatz, S. H. (1990). Synchronization of pulse coupled biological oscillators. *SIAM J. Appl. Math., 50*, 1645–1662.

Morris, C., & Lecar, H. (1981). Voltage oscillations in the barnacle giant muscle fiber. *Biophys. J., 35*, 193–213.

Murakoshi, T., Guo, J., & Ichinose, T. (1993). Electrophysiological identification of horizontal synaptic connections in rat visual cortex in vitro. *Neurosci. Lett., 163*, 211–214.

Nagumo, J., Arimoto, S., & Yoshizawa, S. (1962). An active pulse transmission line simulating nerve axon. *Proc. IRE, 50*, 2061–2070.

Niebur, E., Schuster, H. G., & Kammen, D. M. (1991). Collective frequencies and metastability in networks of limit-cycle oscillators with time delay. *Phys. Rev. Lett., 67*, 2753–2756.

Phillips, W. A., & Singer, W. (1997). In search of common foundations for cortical computation. *Behav. Brain Sci., 20*, 657–722.

Press, W. H., Teukolsky, S. A., Vetterling, W. T., & Flannery, B. P. (1992). *Numerical recipes in C* (2nd ed.). New York: Cambridge University Press.

Singer, W., & Gray, C. M. (1995). Visual feature integration and the temporal correlation hypothesis. *Ann. Rev. Neurosci., 18*, 555–586.

Somers, D., & Kopell, N. (1993). Rapid synchrony through fast threshold modulation. *Biol. Cybern., 68*, 393–407.

Terman, D., & Wang, D. L. (1995). Global competition and local cooperation in a network of neural oscillators. *Physica D, 81*, 148–176.

Traub, R., Whittington, M., Stanford, M., & Jefferys, J. (1996). A mechanism for generation of long-range synchronous fast oscillations in the cortex. *Nature, 383*, 621–624.

van Vreeswijk, C., Abbott, L. F., & Ermentrout, B. (1994). When inhibition not excitation synchronizes neural firing. *J. Comp. Neurosci., 1*, 313–321.

Wang, D. L. (1995). Emergent synchrony in locally coupled neural oscillators. *IEEE Trans. Neural Net., 6(4)*, 941–948.

Wang, D. L. (1999). Relaxation oscillators and networks. In J. Webster (Ed.), *Encyclopedia of electrical and electronic engineers* (vol. 18, pp. 396–405). New York: Wiley.

Wirkus, S., & Rand, R. (1997). Dynamics of two coupled van der Pol oscillators with delay coupling. In *Proceedings of ASME Design Engineering Technical Conference*.

Young, J. F., Wood, B. M., Liu, H. C., Buchanan, M., Landheer, D., Spring, A. J., Thorpe, A., & Mandeville, P. (1988). Effect of circuit oscillations on the DC current-voltage characteristics of double barrier resonant tunneling devices. *Appl. Phys. Lett., 52*, 1398–1401.

Received November 8, 1999; accepted July 20, 2000.